ISSN 0915-633X

NATIONAL INSTITUTE FOR FUSION SCIENCE

Baroclinic Vortex Generation by a Comet Shoemaker-Levy 9 Impact

E. Matsunaga, T.Yabe and M. Tajima

(Received - Aug.4, 1997)

NIFS-509 Sep. 1997

RESEARCH REPORT
NIFS Series

NAGOYA, JAPAN

Baroclinic Vortex Generation by a Comet Shoemaker-Levy 9 Impact

E.Matsunaga, T.Yabe, and M.Tajima

Department of Energy Sciences, Tokyo Institute of Technology, 4259 Nagatsuta, Midori-ku, Yokohama 226, Japan

Abstract

Impact of Shoemaker-Levy 9 caused various changes on Jupiter. One of them is the comet impact sites left on the surface of Jupiter. These impact sites were very stable and long-lived, which is a mystery worthy for detailed investigation. One hypothesis that is most probable one is to attribute these stable structures to vortex. Then a question arises when the vortex is generated. This paper shows that quite a large vortex can be generated by baroclinic mechanism which is caused by non-parallel density and pressure gradients during the break-up of the comet in Jovian atmosphere. The size of the vorticity thus generated is consistent with the size of comet impact sites under Kelvin's circulation theorem.

Keywords : Comet, SL9, Vortex, Simulation

Introduction

On July 1994, the comet Shoemaker-Levy 9 crashed with Jupiter(Shoemaker et al., 1993). In consequence of the impact, various changes occurred on Jupiter. Among those changes, D/G comet impact sites left on the Jupiter surface are one of mysterious events(Hammel et al., 1995). These impact sites were very stable, and were observed on Jupiter for over a month. Such stable and long-lived structures may be attributed to vortices. Then question arises how these vortices are generated during the process of comet impact in Jovian atmosphere. In this paper, we present simulation results that indicate the possibility of vortex generation.

Break-Up Calculation

If the vortex should have been generated, it can be attributed to some change of the comet Shoemaker-Levy 9 in Jovian atmosphere. Therefore it is natural to start with the process of the comet break-up in Jovian atmosphere(Ahrens et al., 1994; Mac Low and Zahnle, 1994; Yabe et al.,1994; Boslough et al., 1994; Yabe et al.,1995).

To carry out the calculation, we used a following simplified model for Jovian atmosphere. Initial profile of pressure was determined from the hydrostatic equilibrium : $\nabla p = \rho g$ with constant temperature. Thus initial pressure and density profiles are $p=p_0 \exp[-(r-r_0)/L]$, $\rho = \rho_0 \exp[-(r-r_0)/L]$, where subscript 0 means some reference point. L is given by $L=p_0/(\rho_0 g)$ with p_0=10bar, $\rho_0=10^{-3}$g/cm^3, g=980×2.37 cm/sec.^{2}, r_0=150km. Jovian atmosphere followed ideal EOS with the specific heat rate of 1.4. The calculation system is taken to be in the moving frame with a velocity of 60km/sec, which is coincident with the entry velocity of SL9.

For the comet, we used the following model. The radius r_c of the comet was changed from 0.125km to 3km. The density of the comet is 1g/cm^3. For the comet, we used the Tait equation(Cole, 1948) : $(p[\text{bar}]+B)/(1+B) = (\rho\,[\text{g/cm}^3]/1)^7$ where B=3000 bar for water and 24000 bar for ice.

We used a cylindrically symmetric coordinate system in two-dimensional calculations and the Cartesian coordinate system in three-dimensional calculation.

Under these conditions, we carried out calculation by hydrodynamic code based on the algorithm CIP(Takewaki et al., 1985; Yabe et al., 1991; Yabe and Wang, 1991; Yabe and Xiao, 1993) .

Figure 1-(a) shows the density contour in the two-dimensional calculation with ice EOS and comet of 3km radius. Time scale is 1.8, 2.7, 3.6 sec. as time fiducial is Jovian atmosphere presure is about 300 mbar. First, the comet lost matter from the front. Around 1.8 sec. , a hole starts to be generated at the front surface of the comet. As the hole gradually grows, it goes through the comet like a tunnel(t= 3.6 sec.). The similar result was obtained by Zahnle's group. Since both result are obtained from axisymmetric

2D simulation, question arises whether a hole is a real consequence or a numerical product at the axial singular point. We have repeated the calculation with 3D Cartesian coordinate and confirmed similar phenomena as shown in Figure 2.

Vortex Generation

There are several mechanisms by which vortex can be generated. One of them is viscosity. Karman vortex is a typical example and is caused by a large velocity shear at the cylinder surface. Once the vortex thus created leaves the surface, it is hardly dissipated because the velocity shear in the main flow is too small to make the viscosity effective. In the present case, however, a shock wave is generated in front of the comet and Karman vortex does not appear.

Another mechanism is not well known but is a baroclinic term. Here we briefly review how the term can be derived by focusing only on the responsible term and neglecting other terms. The equation of motion corresponding to the term is

$$\frac{\partial \mathbf{u}}{\partial t} = -\frac{1}{\rho}\nabla p \qquad (1)$$

Taking the rotation of equation (1), we get

$$\frac{\partial \omega}{\partial t} = \frac{1}{\rho^2}(\nabla \rho) \times (\nabla p) \qquad (2)$$

where $\omega(\equiv \nabla \times \mathbf{u})$ is the vorticity. Thus, the vortex can be generated by non-parallel p and ρ gradients. If the fluid is barotropic gas $p = p(\rho)$, then $(\nabla\rho) \times (\nabla p) = (\nabla\rho \times \nabla\rho) \cdot (dp / d\rho) = 0$ and no vortex is generated. In this sense, the baroclinic term may be considered to be not responsible for the vortex generation and dissipation in ordinary situation. However, we show in this paper that the term can be large enough during a break-up of Shoemaker-Levy 9.

Now, we investigate vorticity change. Figure 1-(b) shows vorticity contour. Each figure displays the same time sequence as Figure 1-(a). According to Fig.1-(a) and Fig.1-(b), it is seen that when Jovian atmospheric jet passes through the comet hole, large vorticity is generated behind the comet (t=3.6sec.). The maximum vorticity at 2.4 sec was typically 100~350/sec.

We repeated the calculation by changing the radius of the comet. Figure 3 shows the summary of the results, where $\int \omega dS$ means the integration of vorticity over the cross section area dS. According to the Kelvin's circulation theorem, $\int \omega dS$ should be conserved if the baroclinic term is absent, which is justified in the undisturbed atmosphere in Jupiter. Thus we can compare $\int \omega dS$ in Fig.3 with the observation data. According to observations (Takeuchi, 1995), the velocity at the impact sites is about V_0 = 100m/sec . If the size of the impact site is D, then vorticity is about $\omega_0 = V_0 / D$. Multiplication by surface area D^2 gives $\int \omega dS = V_0 \cdot D$.

By using this relation and adopting V_0=100m/sec from the observation, we estimated the size of the impact site as show in Fig. 3. Interestingly, $\int \omega dS$ and the size of impact sites linearly increase as the radius r_c of the comet for $r_c \le 1km$ and abruptly jump at $r_c \approx 1.5km$ staying to be a constant value for $r_c > 1.5km$. The constant value is 3000 km which is consistent with the observation.

Summary

In this paper, we have shown one of the mechanisms for generating vorticity that is large enough to explain the observation data of impact sites caused by SL9 impact. During a break-up process in Jovian atmosphere, a hole is created along the axis of the comet and finally penetrates through the comet causing large vortex ring at the rear end of the comet. Since the area weighted vorticity is conserved according to the Kelvin's circulation theorem, we estimated the size of the impact site, which agrees with observation data.

This work was carried out under the collaborating research program at the National Institute for Fusion Science of Japan.

References

Ahrens, T.J., T.Takata, J.D.O'Keefe, and G.S.Orton, Impact of Comet Shoemaker-Levy 9 on Jupiter, Geop.Res.Lett,1087-1090, 1994.

Boslough, M.B., D.A.Crawford, A.C.Robinson, and T.G.Trucano, Mass and Penetration Depth of Shoemaker-Levy 9 Fragments from Time-Resolved Photometry, Geophys.Res.Lett. 21, 1555-1558, 1994.

Cole, R.H., *Underwater Explosions*, Princeton University Press, Princeton NJ, 1948.

Hammel, H.B. et al., Hubble Space Telescope imaging of Jupiter:Atmospheric phenomena created by the impact of Comet Shoemaker-Levy 9, Science, 267,1288-1296, 1995.

Mac Low, M. and K.Zahnle, Explosion of Comet Shoemaker-Levy 9 on Entry into the Jovian Atmosphere, Ap.J.,434,L33-L36, 1994.

Shoemaker, C.S., E.M.Shoemaker, and D.H.Levy, Comet Sheomaker-Levy , IAU Circ.,5725, 1993.

Takeuchi, S., KAGAKU., vol.65,no.11,752-756, 1995.

Takewaki, H., A.Nishiguchi, and T.Yabe, The Cubic-Interpolated Pseudo-Particle (CIP) Method for Solving Hyperbolic-Type Equations,J.Comput.Phys.,61,261-268, 1985.

Yabe, T. et al., A Universal Solver for Hyperbolic Equations by Cubic-Polynomial Interpolation, Comput.Phys.Comm., 66,219 -

242, 1991.

Yabe, T. and P.Y.Wang, Unified Numerical Procedure for Compressible and Incompressible Fluid,J.Phys.Soc.Japan, 60,2105-2108, 1991.

Yabe, T. and F.Xiao, Description of Complex and Sharp Interface during Shock Wave Interaction with Liquid Drop, J.Phys.Soc. Japan, 62,2537-2540, 1993.

Yabe, T., F.Xiao, D.Zhang, S,Sasaki, Y.Abe, N.Kobayashi and T.Terasawa, Effect of EOS on Break-Up of Shoemaker-Levy 9 Entering Jovian Atmosphere, J.Geomag.Geoelectr.,46,657-662,1994.

Yabe, T., T.Aoki, M.Tajima, F.Xiao, S.Sasaki,Y.Abe and J.Watanabe, Possible Explanation of the Secondary Flash and Strong Flare on IR Lightcurves upon Impact of Shoemaker-Levy 9, Geop.Res.Lett., vol.22,no.17,2429-2432,1995.

Figure Captions

Fig.1-a) : The density contour in the axisymmetric 2D calculation with ice EOS and comet radius 3km.

Fig.1-b) : The vorticity contour in the axisymmetric 2D calculation with ice EOS and comet radius 3km.

Fig.2 : The density contour in the 3D calculation with Cartesian coordinate with ice EOS.

Fig.3 : Dependence of generated circulation on the radius of the comet and estimated impact sites size from the Kelvin's circulation theorem.

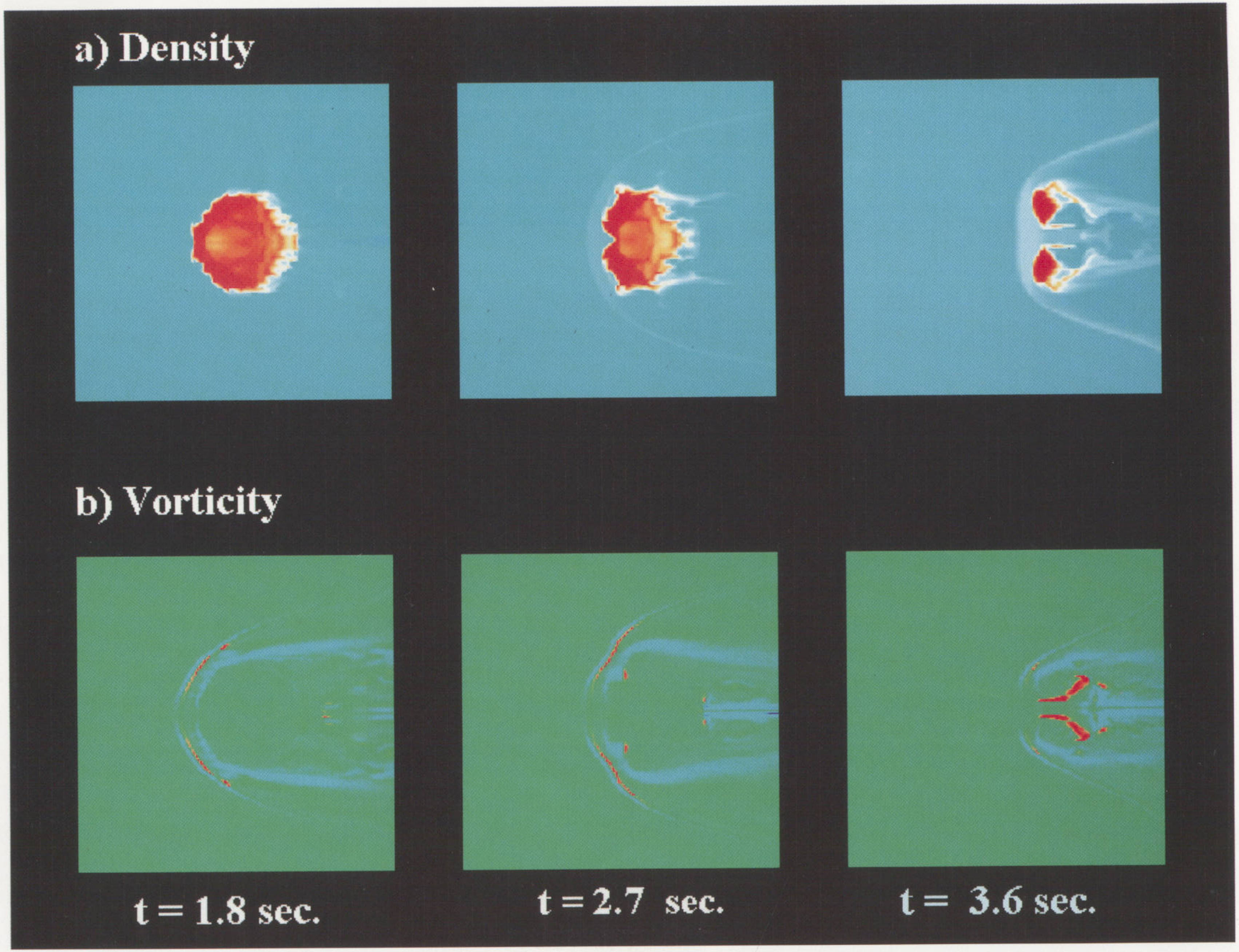

Fig. 1

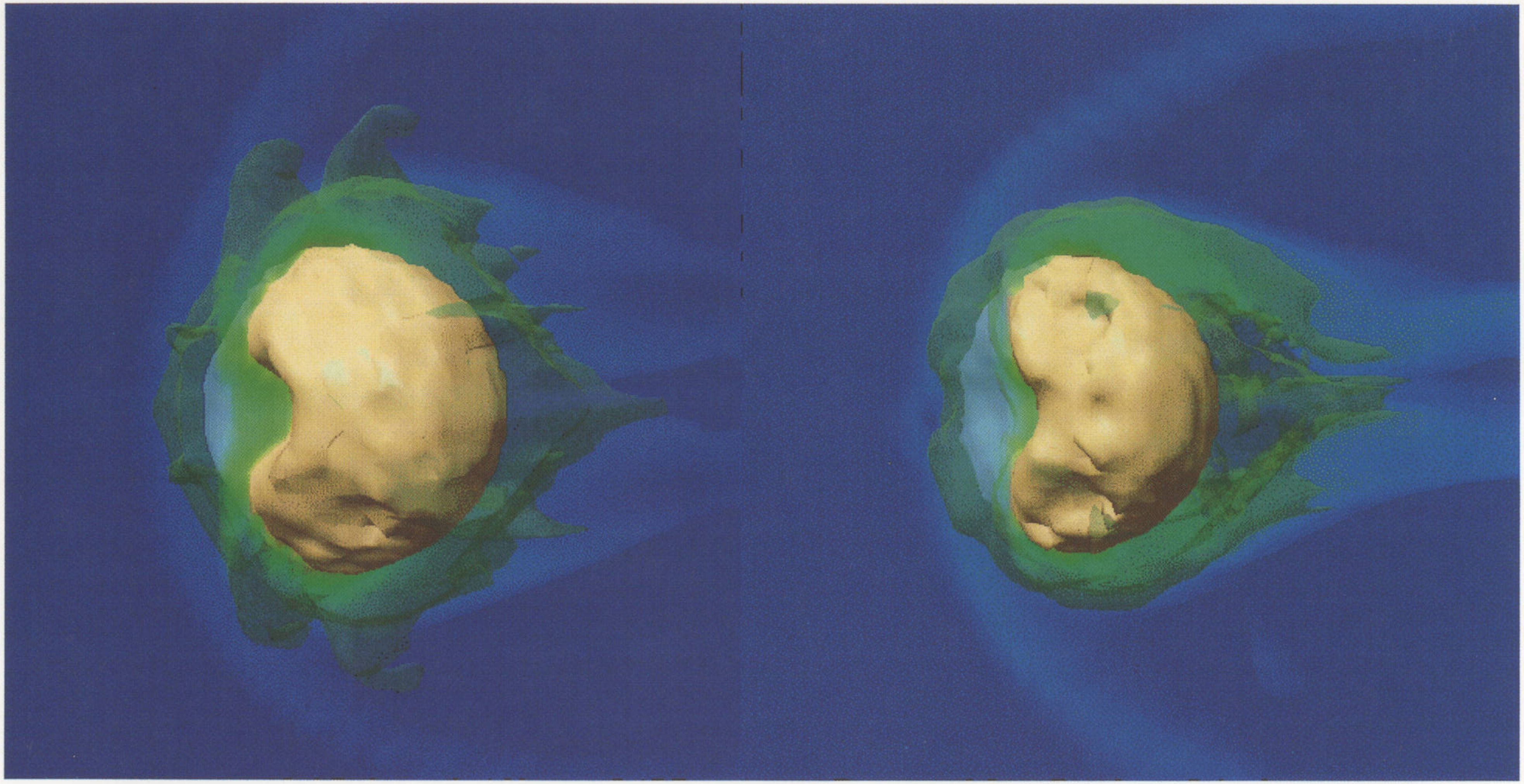

Fig.2

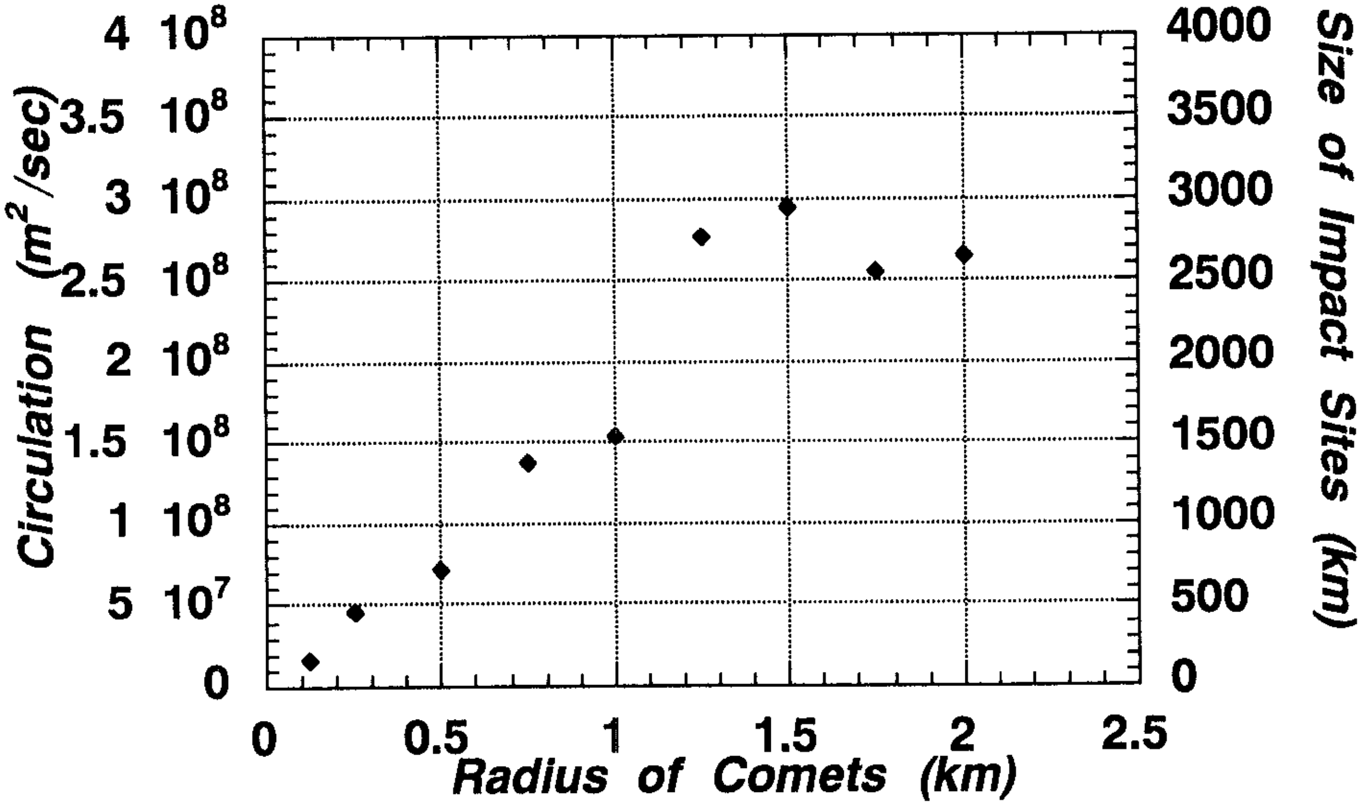

Circulation (m²/sec)
4 10⁸
3.5 10⁸
3 10⁸
2.5 10⁸
2 10⁸
1.5 10⁸
1 10⁸
5 10⁷
0
0
0.5
1
1.5
2
2.5
Radius of Comets (km)
Size of Impact Sites (km)
4000
3500
3000
2500
2000
1500
1000
500
0

Fig. 3

Recent Issues of NIFS Series

NIFS-462 N. Katsuragawa, H. Hojo and A. Mase,
Simulation Study on Cross Polarization Scattering of Ultrashort-Pulse Electromagnetic Waves; Nov. 1996

NIFS-463 V. Voitsenya, V. Konovalov, O. Motojima, K. Narihara, M. Becker and B. Schunke,
Evaluations of Different Metals for Manufacturing Mirrors of Thomson Scattering System for the LHD Divertor Plasma; Nov. 1996

NIFS-464 M. Pereyaslavets, M. Sato, T. Shimozuma, Y. Takita, H. Idei, S. Kubo, K. Ohkubo and K. Hayashi,
Development and Simulation of RF Components for High Power Millimeter Wave Gyrotrons; Nov. 1996

NIFS-465 V.S. Voitsenya, S. Masuzaki, O. Motojima, N. Noda and N. Ohyabu,
On the Use of CX Atom Analyzer for Study Characteristics of Ion Component in a LHD Divertor Plasma; Dec. 1996

NIFS-466 H. Miura and S. Kida,
Identification of Tubular Vortices in Complex Flows; Dec. 1996

NIFS-467 Y. Takeiri, Y. Oka, M. Osakabe, K. Tsumori, O. Kaneko, T. Takanashi, E. Asano, T. Kawamoto, R. Akiyama and T. Kuroda,
Suppression of Accelerated Electrons in a High-current Large Negative Ion Source; Dec. 1996

NIFS-468 A. Sagara, Y. Hasegawa, K. Tsuzuki, N. Inoue, H. Suzuki, T. Morisaki, N. Noda, O. Motojima, S. Okamura, K. Matsuoka, R. Akiyama, K. Ida, H. Idei, K. Iwasaki, S. Kubo, T. Minami, S. Morita, K. Narihara, T. Ozaki, K. Sato, C. Takahashi, K. Tanaka, K. Toi and I. Yamada,
Real Time Boronization Experiments in CHS and Scaling for LHD; Dec. 1996

NIFS-469 V.L. Vdovin, T.Watari and A. Fukuyama,
3D Maxwell-Vlasov Boundary Value Problem Solution in Stellarator Geometry in Ion Cyclotron Frequency Range (final report); Dec. 1996

NIFS-470 N. Nakajima, M. Yokoyama, M. Okamoto and J. Nührenberg,
Optimization of M=2 Stellarator; Dec. 1996

NIFS-471 A. Fujisawa, H. Iguchi, S. Lee and Y. Hamada,
Effects of Horizontal Injection Angle Displacements on Energy Measurements with Parallel Plate Energy Analyzer; Dec. 1996

NIFS-472 R. Kanno, N. Nakajima, H. Sugama, M. Okamoto and Y. Ogawa,
Effects of Finite-β and Radial Electric Fields on Neoclassical Transport in the Large Helical Device; Jan. 1997

NIFS-473 S. Murakami, N. Nakajima, U. Gasparino and M. Okamoto,
Simulation Study of Radial Electric Field in CHS and LHD; Jan. 1997

NIFS-474 K. Ohkubo, S. Kubo, H. Idei, M. Sato, T. Shimozuma and Y. Takita,
Coupling of Tilting Gaussian Beam with Hybrid Mode in the Corrugated Waveguide; Jan. 1997

NIFS-475 A. Fujisawa, H. Iguchi, S. Lee and Y. Hamada,
Consideration of Fluctuation in Secondary Beam Intensity of Heavy Ion Beam Prove Measurements; Jan. 1997

NIFS-476 Y. Takeiri, M. Osakabe, Y. Oka, K. Tsumori, O. Kaneko, T. Takanashi, E. Asano. T. Kawamoto, R. Akiyama and T. Kuroda,
Long-pulse Operation of a Cesium-Seeded High-Current Large Negative Ion Source; Jan. 1997

NIFS-477 H. Kuramoto, K. Toi, N. Haraki, K. Sato, J. Xu, A. Ejiri, K. Narihara, T. Seki, S. Ohdachi, K. Adati, R. Akiyama, Y. Hamada, S. Hirokura, K. Kawahata and M. Kojima,
Study of Toroidal Current Penetration during Current Ramp in JIPP T-IIU with Fast Response Zeeman Polarimeter; Jan., 1997

NIFS-478 H. Sugama and W. Horton,
Neoclassical Electron and Ion Transport in Toroidally Rotating Plasmas; Jan. 1997

NIFS-479 V.L. Vdovin and I.V. Kamenskij,
3D Electromagnetic Theory of ICRF Multi Port Multi Loop Antenna; Jan. 1997

NIFS-480 W.X. Wang, M. Okamoto, N. Nakajima, S Murakami and N. Ohyabu,
Cooling Effect of Secondary Electrons in the High Temperature Divertor Operation; Feb. 1997

NIFS-481 K. Itoh, S.-I. Itoh, H. Soltwisch and H.R. Koslowski,
Generation of Toroidal Current Sheet at Sawtooth Crash; Feb. 1997

NIFS-482 K. Ichiguchi,
Collisionality Dependence of Mercier Stability in LHD Equilibria with Bootstrap Currents; Feb. 1997

NIFS-483 S. Fujiwara and T. Sato,
Molecular Dynamics Simulations of Structural Formation of a Single Polymer Chain: Bond-orientational Order and Conformational Defects; Feb. 1997

NIFS-484 T. Ohkawa,
Reduction of Turbulence by Sheared Toroidal Flow on a Flux Surface; Feb. 1997

NIFS-485 K. Narihara, K. Toi, Y. Hamada, K. Yamauchi, K. Adachi, I. Yamada, K. N. Sato, K.

Kawahata, A. Nishizawa, S. Ohdachi, K. Sato, T. Seki, T. Watari, J. Xu, A. Ejiri, S. Hirokura, K. Ida, Y. Kawasumi, M. Kojima, H. Sakakita, T. Ido, K. Kitachi, J. Koog and H. Kuramoto,
Observation of Dusts by Laser Scattering Method in theJIPPT-IIU Tokamak
Mar. 1997

NIFS-486 S. Bazdenkov, T. Sato and The Complexity Simulation Group,
Topological Transformations in Isolated Straight Magnetic Flux Tube; Mar. 1997

NIFS-487 M. Okamoto,
Configuration Studies of LHD Plasmas; Mar. 1997

NIFS-488 A. Fujisawa, H. Iguchi, H. Sanuki, K. Itoh, S. Lee, Y. Hamada, S. Kubo, H. Idei, R. Akiyama, K. Tanaka, T. Minami, K. Ida, S. Nishimura, S. Morita, M. Kojima, S. Hidekuma, S.-I. Itoh, C. Takahashi, N. Inoue, H. Suzuki, S. Okamura and K. Matsuoka,
Dynamic Behavior of Potential in the Plasma Core of the CHS Heliotron/Torsatron; Apr. 1997

NIFS-489 T. Ohkawa,
Pfirsch - Schlüter Diffusion with Anisotropic and Nonuniform Superthermal Ion Pressure; Apr. 1997

NIFS-490 S. Ishiguro and The Complexity Simulation Group,
Formation of Wave-front Pattern Accompanied by Current-driven Electrostatic Ion-cyclotron Instabilities; Apr. 1997

NIFS-491 A. Ejiri, K. Shinohara and K. Kawahata,
An Algorithm to Remove Fringe Jumps and its Application to Microwave Reflectometry; Apr. 1997

NIFS-492 K. Ichiguchi, N. Nakajima, M. Okamoto,
Bootstrap Current in the Large Helical Device with Unbalanced Helical Coil Currents; Apr. 1997

NIFS-493 S. Ishiguro, T. Sato, H. Takamaru and The Complexity Simulation Group,
V-shaped dc Potential Structure Caused by Current-driven Electrostatic Ion-cyclotron Instability; May 1997

NIFS-494 K. Nishimura, R. Horiuchi, T. Sato,
Tilt Stabilization by Energetic Ions Crossing Magnetic Separatrix in Field-Reversed Configuration; June 1997

NIFS-495 T. -H. Watanabe and T. Sato,
Magnetohydrodynamic Approach to the Feedback Instability; July 1997

NIFS-496 K. Itoh, T. Ohkawa, S. -I.Itoh, M. Yagi and A. Fukuyama
Suppression of Plasma Turbulence by Asymmetric Superthermal Ions; July 1997

NIFS-497 T. Takahashi, Y. Tomita, H. Momota and Nikita V. Shabrov,
Collisionless Pitch Angle Scattering of Plasma Ions at the Edge Region of an FRC; July 1997

NIFS-498 M. Tanaka, A.Yu Grosberg, V.S. Pande and T. Tanaka,
Molecular Dynamics and Structure Organization in Strongly-Coupled Chain of Charged Particles; July 1997

NIFS-499 S. Goto and S. Kida,
Direct-interaction Approximation and Reynolds-number Reversed Expansion for a Dynamical System; July 1997

NIFS-500 K. Tsuzuki, N. Inoue, A. Sagara, N. Noda, O. Motojima, T. Mochizuki, T. Hino and T. Yamashina,
Dynamic Behavior of Hydrogen Atoms with a Boronized Wall; July 1997

NIFS-501 I. Viniar and S. Sudo,
Multibarrel Repetitive Injector with a Porous Pellet Formation Unit; July 1997

NIFS-502 V. Vdovin, T. Watari and A. Fukuyama,
An Option of ICRF Ion Heating Scenario in Large Helical Device; July 1997

NIFS-503 E. Segre and S. Kida,
Late States of Incompressible 2D Decaying Vorticity Fields; Aug. 1997

NIFS-504 S. Fujiwara and T. Sato,
Molecular Dynamics Simulation of Structural Formation of Short Polymer Chains; Aug. 1997

NIFS-505 S. Bazdenkov and T. Sato
Low-Dimensional Model of Resistive Interchange Convection in Magnetized Plasmas; Sep. 1997

NIFS-506 H. Kitauchi and S. Kida,
Intensification of Magnetic Field by Concentrate-and-Stretch of Magnetic Flux Lines; Sep. 1997

NIFS-507 R.L. Dewar,
Reduced form of MHD Lagrangian for Ballooning Modes; Sep. 1997

NIFS-508 Y.-N. Nejoh,
Dynamics of the Dust Charging on Electrostatic Waves in a Dusty Plasma with Trapped Electrons; Sep.1997

NIFS-509 E. Matsunaga, T.Yabe and M. Tajima,
Baroclinic Vortex Generation by a Comet Shoemaker-Levy 9 Impact; Sep. 1997